Spring 5-31-2009

Experimental investigation of mixing time in a stirred, torispherical-bottomed tank equipped with a retreat-blade impeller

Nonjaros Chomcharn
New Jersey Institute of Technology

Recommended Citation

Chomcharn, Nonjaros, "Experimental investigation of mixing time in a stirred, torispherical-bottomed tank equipped with a retreat-blade impeller" (2009). *Theses*. 306.
https://digitalcommons.njit.edu/theses/306

ABSTRACT

EXPERIMENTAL INVESTIGATION OF MIXING TIME IN A STIRRED, TORISPHERICAL-BOTTOMED TANK EQUIPPED WITH A RETREAT-BLADE IMPELLER

by
Nonjaros Chomcharn

Glass-lined reactors are typically used in the pharmaceutical and specialty chemicals industries because of their material compatibility with most reactants and their cleanability. These reactors are typically equipped with a retreat-blade impeller placed close to the bottom of the tank a single baffle mounted from the top. The mixing performance of such reactors has not received significant attention in the literature, despite their ubiquitous presence in the pharmaceutical industry. In particular, mixing time, i.e., the time required by the system to achieve a predefined level of homogeneity, has not been studied to any significant degree.

In this work, the mixing time in a 60-L, scaled-down version of an actual industrial reactor having an industrial-type torispherical bottom and equipped with a retreat-blade impeller was experimentally determined for three different baffling configurations, i.e., unbaffled tank, partially baffled tank (in which the typical beavertail baffle was used), and fully baffled tank (i.e., with four full baffles). A conductivity method using sodium chloride (NaCl) as a tracer was used as one the main method to determine mixing time. Experiments in the unbaffled system were conducted by installing one two probes in the mixing vessel (at the wall and midway between the wall and the shaft, respectively). The presence of the conductivity probe(s) had a significant impact on mixing time. Results showed that different mixing times were obtained with the conductivity method depending on the location of the probe(s) and the number of

probes. A separate colorimetric method coupled with image processing was additionally used to determine the mixing time. Both methods produced similar results when two probes were present, probably because of the baffling effects introduced by the probes themselves.

Results were also obtained for the partial baffled system and the fully baffled system, but only using the conductivity method. Experiments were performed when the agitation speed was varied in order to establish a correlation between mixing time and rotational speed for all systems. The mixing time in the partially baffled system was found to decrease with increasing impeller speeds and the predicted mixing time from regression agreed well with the experimental results. As for the fully baffled system, the mixing time varied in inverse proportion to the agitation speed, as in the typical baffled systems. The non-dimensional mixing number, $\theta_{95}N$, was obtained within the speed range of 100–200 rpm for both the partially baffled and the baffled system. In the latter case, $\theta_{95}N$ was found to be independent of impeller speed, as expected.

EXPERIMENTAL INVESTIGATION OF MIXING TIME IN A STIRRED, TORISPHERICAL-BOTTOMED TANK EQUIPPED WITH A RETREAT-BLADE IMPELLER

by
Nonjaros Chomcharn

A Thesis
Submitted to the Faculty of
New Jersey Institute of Technology
in Partial Fulfillment of the Requirements for the Degree of
Master of Science in Pharmaceutical Engineering

Otto H. York Department of Chemical, Biological and Pharmaceutical Engineering

May 2009

APPROVAL PAGE

EXPERIMENTAL INVESTIGATION OF MIXING TIME IN A STIRRED, TORISPHERICAL-BOTTOMED TANK EQUIPPED WITH A RETREAT-BLADE IMPELLER

Nonjaros Chomcharn

May 12, 2009

Dr. Piero M. Armenante, Thesis Advisor Date
Distinguished Professor of Chemical, Biological and Pharmaceutical Engineering, NJIT

5/12/09

Dr. Laurent Simon, Committee Member Date
Associate Professor of Chemical, Biological and Pharmaceutical Engineering, NJIT

5/12/09

Dr. Robert B. Barat, Committee Member Date
Professor of Chemical, Biological and Pharmaceutical Engineering, NJIT

BIOGRAPHICAL SKETCH

Author: Nonjaros Chomcharn

Degree: Master of Science

Date: May 2009

Undergraduate and Graduate Education:

- Master of Science in Pharmaceutical Engineering,
  New Jersey Institute of Technology, Newark, NJ, 2009
- Bachelor of Science in Pharmaceutical Science,
  Chulalongkorn University, Bangkok, Thailand, 2003

Major: Pharmaceutical Engineering

You may be disappointed if you fail, but you are doomed if you don’t try.
Beverly Sills

ACKNOWLEDGMENT

I would like to express my deepest appreciation to Dr. Piero M. Armenante, who not only served as my research advisor, providing valuable and countless resources, insight, and intuition, but also constantly gave me support, encouragement, and reassurance. Special thanks are given to Dr. Robert B. Barat, Dr. Laurent Simon for actively participating in my committee.

I would like to specially thank Giuseppe Di Benedetto and Micaela Caramellino, Shilan Motamedvaziri, and Yimin Wang for their continuous support throughout my research. I cannot end without thanking my family especially my parents, on whose constant encouragement and love I have relied throughout my academic career. I dedicate this thesis to them.

TABLE OF CONTENTS

TABLE OF CONTENTS
(Continued)

Chapter **Page**

LIST OF TABLES

LIST OF FIGURES

LIST OF FIGURES
(Continued)

LIST OF FIGURES
(Continued)

NOMENCLATURE

D	impeller diameter (m)
T	tank diameter (m)
H	liquid height (m)
C	bottom clearance (m)
N	rotational speed (rpm)
Re	Reynolds number
ρ	liquid density (kg/m^3)
μ	liquid viscosity (m^2/s)
θ_D	mixing time to achieve a desired level (s)
θ_{95}	mixing time to achieve a 95% uniformity level (s)

CHAPTER 1

INTRODUCTION

1.1 Background

Stirred glass-line reactors are commonly used in the chemical and pharmaceutical industries. A typical glass-lined reactor is equipped with a retreat-blade impeller close to the bottom and a single baffle. Glass lining provides corrosion resistance, ease of cleanliness, and reduces product contamination [1], but it often requires manufacturing the agitation system and the tank so that no baffles are present in the tank. Instead, some baffling is provided by inserting a single baffle from the reactor roof. Without baffling or with insufficient baffling , the fluid moves in a swirling motion in the tank creating a central vortex, and mixing is inefficient [2]. Installing baffles eliminates such swirling motion by breaking a vortex and ultimately improving the mixing process.

A standard baffling configuration in most mixing tanks consists of four vertical plates having width equal to 8 to 10% (T/12 to T/10) of the tank diameter [3] and mounted at the tank wall. Wall baffles have drawback since of cleaning can be more difficult than in an unbaffled tank, which is critical in pharmaceutical products. This is why a single baffle, typically a beavertail baffle, is preferred in glass-lined reactors. The beavertail baffle is typically mounted through a nozzle in the vessel head because to mounting to the side of a glass-lined vessel is difficult or impossible [1]. In recent years, new glass-lined impeller designs have been made available by manufacturers. However, a few studies on performance characteristics of these impellers and configurations are available.

Mixing time is one of the most important factors associated with the mixing performance of an agitation system. Mixing time (also know as blend time) is defined as the time required to reach a predefined degree of homogeneity [3]. There are several methods which can be used to determine mixing time, both qualitatively and quantitatively. The conductivity method, one of the quantitative methods, can measure the mixing time by tracing the concentration of an electrolyte added to the liquid in the tank [3]. This technique is simple and does not require a complicated data acquisition system. However, a conductivity probe is inevitably inserted in the vessel in order to measure conductivity and this may change the flow in the system. Therefore, the size of the probe should minimize as much as possible to avoid disturbance in the system. The colorimetric method is an alternative method to determine mixing time non-intrusively. The colorimetric method is typically used to measure the approximate mixing time by visual inspection at a definite monitoring point. Currently, image processing of digitized images of the mixing system when a color tracer is added can be used, in combination with imaging processing software, to detect a color change at a particular location in the vessel very precisely. Applying image processing to the colorimetric method, one can determine the mixing time at each particular point by monitoring color evolution after the mixing process is initiated. Cabaret et al. [4] have studied this approach and concluded that this method is highly reproducible and can identify unmixed zones.

1.2 Objectives of This Work

The objective of this work is to experimentally determine the mixing time under different operating conditions for a glass-lined type of tank with a torispherical bottom and equipped with a retreat-blade impeller and different baffling configurations. The configuration of the system used here is based on the previous work of Giuseppe Di Benedetto, a former student in this lab. Two experimental methods were used in the current work to determine mixing time, i.e., a conductivity method and a colorimetric method were used. When conductivity probes are placed in the tank, the probes will affect the local mixing by changing the flow pattern, especially if the system in unbaffled. Therefore, a colorimetric method was developed to confirm the mixing time data obtained with the conductivity measurements.

This work also investigated the effect of operating parameters such as agitation speed on mixing time, in order to establish a correlation between mixing time and the agitation speed in unbaffled, partially baffled and fully baffled mixing systems.

CHAPTER 2

EXPERIMENTAL APPARATUS AND METHOD

2.1 Mixing Tank and Agitation System

2.1.1 Mixing Tank

In this work, a cylindrical tank with a torispherical dish bottom was used as the mixing tank. This tank was commissioned, and paid for, by Eli Lilly (thanks to Dr. Billy Allen, Eli Lilly, Indianapolis, IN). The tank was fabricated through the BHR Group in the UK (with Dr. David Brown's assistance) explicitly for this work. The tank was made of a thin (0.5 mm) fluorinated ethylene propylene co-polymer (FEP) rigid film. This material has a refractive index of 1.338, i.e., very similar to that of water (1.333) in order to minimize any curvature effect during the experiments and in the subsequent image processing step. The tank diameter, T, was 450 mm and its total height was 540 mm. The height of the dish bottom section was 155 mm. The tank had a rigid collar and lip at its top so that it could be suspended in a larger "host" square tank, as shown in Figure 2.1. During an experiment, the mixing tank was placed in such as square Plexiglas tank and both the mixing tank and the square tank were filled with liquid at about the same height in order to eliminate any differential pressure across the thin wall of the mixing tank that would have ruptured it. In all cases, the liquid height to tank diameter ratio, H/T, was always equal to one, corresponding to a liquid volume of 60,488 cm^3.

2.1.2 Agitation System

A typical single three-blade retreat-blade curved impeller, similar to those routinely used in the pharmaceutical industry in glass-lined vessels, was used in all experiments. The impeller dimensions were measured with a caliper and were as follow: impeller diameter, D = 219.1 mm; radius of curvature of the blades = 92.08 mm; height of the blade = 25.4 mm; and thickness of the blade = 12.7 mm. This impeller was a scaled down version of a commercial, industrial De Dietrich impeller, as further discussed below. This impeller was kindly donated by Dr. San Kiang of Bristol-Myers Squibb, New Brunswick, NJ. In all experiments, the impeller diameter-to-tank diameter ratio, D/T, was always 0.489 and the impeller clearance off the tank bottom, C, was 40 mm, corresponding to $C/T = 0.183$. These ratios were used in previous work by this group and were based on the design of a scale-down impeller manufactured by the De Dietrich company, a leading manufacturer of glass-lined equipment and accessories for the pharmaceutical and chemical industries (specifications were kindly provided by Eric Momsen, Process Engineer, for De Dietrich Company, Union, NJ). The impeller was attached to the end of a shaft having a diameter of 12.52mm and centrally located inside the tank. The impeller was connected to a 1/4-HP motor (Chemglass, Model CG-2033-11) controlled by an external controller (Chemglass, Model CG-2033-31). The tank was operated completely unbaffled, partially baffled, or fully baffled. For the partially baffled tank, a single beaver-tail baffle shown in Figure 2.1 (b) was used. The dimensions of the baffle were as follows: diameter of the top section, 15.24 mm; length of the top section, 70.64 mm; diameter of the middle section, 22.23 mm; length of the middle section, 199.7 mm; diameter of the bottom section 20.07 mm; length of the bottom section 70.64 mm. The baffle clearance was

90.23 mm from the vessel bottom and 21.38 mm from the top of the impeller to the baffle bottom. The distance from center of the baffle to the wall was 70.3 mm. For the fully baffled tank shown in Figure 2.1(c), the baffles were made of 4 vertical metal plates were mounted from the top. Each metal plate was attached to an acrylic plate in order to increase the width of the baffle. The total width of the baffle was 45 mm and the length of the submerged part was 300 mm measured from the liquid surface.

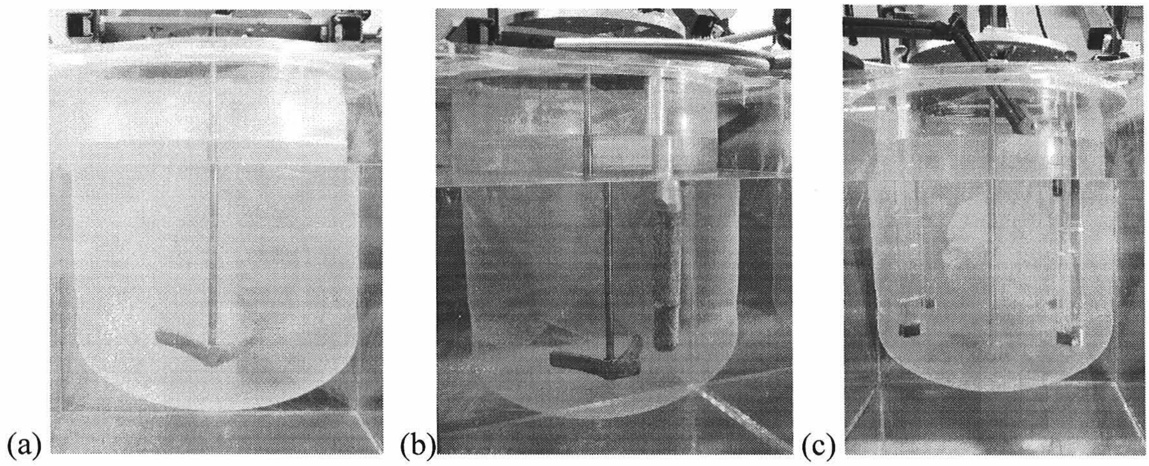

Figure 2.1 Mixing system used in this work:
(a) unbaffled tank
(b) partially baffled tank with beavertail baffle
(c) fully baffled tank

2.2 Materials

Distilled water was always used as the liquid in the mixing tank, which was always filled up to a height, T, equal to the inside tank diameter, i.e., 450 mm (H/T = 1.0). The external rectangular tank was filled with tap water.

2.3 Mixing Time Determination Using Conductivity Measurements

Conductivity measurements of mixing time were taken in the unbaffled, the partially baffled, and the fully baffled systems (in fact this was the only method used in the partially baffled and fully baffled systems). Mixing time experiments were performed by measuring the concentration vs. time history when a solution of a salt (NaCl) tracer was added to the stirred liquid in the tank. In all experiments, a 10-mL solution of sodium chloride (0.85% w/v) in a syringe provided with a cannula (ID: 1mm) was rapidly injected some 5 cm below the liquid surface inside the vessel, adjacent to the shaft. In order to measure the NaCl concentration as a function of time one or two conductivity probes (DuraProbe™ 013005MD conductivity cell, Orion) were used. The conductivity probes were cylindrical and had a diameter equal to 15.3 mm. Regardless of probe position and number of probes, the location of the probe(s) was at the water surface, and the submerged portion of the probe(s) was approximately 8 cm. In the experiments with one probe, the probe was placed either near the wall (15 mm from the wall) or midway between the wall and the shaft (112.5 mm from the wall). In all the experiments in the partially baffled and fully baffled tank only one probe was and used the probe was located behind the beavertail baffle and the wall baffle respectively, which are likely to be poorly mixed regions. In the experiments using two conductivity probes simultaneously, the second probe was located midway between the wall and the shaft (112.5 mm from the wall).

Each probe was connected to a conductivity meter (Orion 3 Stars Conductivity Benchtop, Orion) which was connected to a computer via RS232 cable (Figure 2.2 (a)). Data acquisition was achieved using the Hyperterminal application of Microsoft Windows (Version 2000) operating system. Conductivity measurements from the probes in the vessel were transmitted to the computer every 5 second which was the minimum data acquisition frequency for the conductivity meter used in this work.

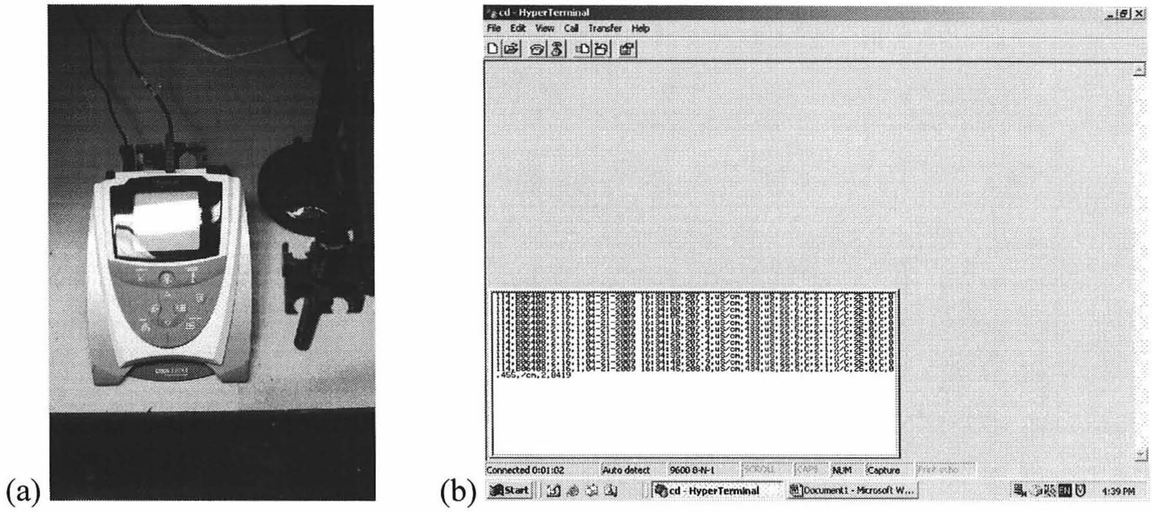

Figure 2.2 Data acquisition system for mixing time determination using conductivity probe technique
(a) conductivity meter (Orion 3 Stars Conductivity Benchtop, Orion)
(b) hyperterminal screen shot as conductivity data was sent from the conductivity meter.

The conductivity data collected by the conductivity probe technique were normalized to eliminate the effect of different probe gains. The data were normalized between an initial zero value measured before the addition of tracer, and a final stable value measured after the test was complete [3]. The normalized output was obtained by

$$C_i' = \frac{C_i - C_0}{C_\infty - C_0} \qquad (1)$$

where C_i' = normalized conductivity probe output
C_i = conductivity at time i
C_∞ = final conductivity (equilibrium)
C_0 = initial conductivity

The mixing time in this work was defined as the time required for the normalized probe output to reach, and then always remain, within ±5% of the final equilibrium value. This time was defined as the 95% mixing time (θ_{95}). According to equation (1), the 95% mixing time was determined at the time when the normalized conductivity output first reached the value of 1 ± 0.05 and then always remained within this interval. Since the conductivity meter only transfer data every 5 seconds, the mixing time could only be determined with an approximation of ±2.5 seconds. To minimize this error, each experiment was conducted in triplicate and the resulting values were averaged.

2.4 Mixing Time Determination Using Colorimetric Measurements and Image Processing

The colorimetric method to determine mixing time was only used in unbaffled tanks. Such mixing time experiments were conducted using a colorimetric technique based on the change in color of an indicator during an acid-base reaction. Phenolphthalein, which is pink when $\text{pH} > 10$ (base color) and colorless when $\text{pH} < 8$ (acid color), was used as the indicator. Prior to the beginning of an experiment, NaOH was added to the distilled water in the tank to make its concentration equal to 10 mol/L ($\text{pH} \cong 11$). The presence of phenolphthalein resulted in an initial pink solution. Then, 10 mL of an 11-mol/L HCl solution were rapidly added at the same surface location as in the conductivity experiments. Each experiment was filmed with a digital video camera (Digital Handycam DCR-TRV740 NTSC, Sony) capturing the color change from pink to colorless at a rate of 30 frames/s. The distance between the tank and the camera was 1.20 m. To obtain a homogenous illumination, a white sheet of paper was placed behind the rectangular vessel as a light diffuser. The digitized images in AVI format were analyzed with the MATLAB application software in order to extract the red, green, and blue (RGB) components of the light intensity at selected, fixed, "sampling" locations on each image. Twenty such locations were selected, as shown in Figure 2.3. For each sampling point, the intensity of the green color component was extracted from each image and plotted as a function of time for a given neutralization experiment. In order to determine the mixing time θ_{95}, the green light intensities were normalized using equation (1). Each experiment was conducted in triplicate and the resulting values were averaged.

In order to minimize the use of distilled water (60 L per batch), at the end of each neutralization experiment the batch was not discarded. Instead, the batch was neutralized with an NaOH solution until the pH was 11, as measured with a pH meter (Orion model 410A). The distilled water was replaced when a new set of variables (without probe, one probe, and 2 probes) were explored, typically every day.

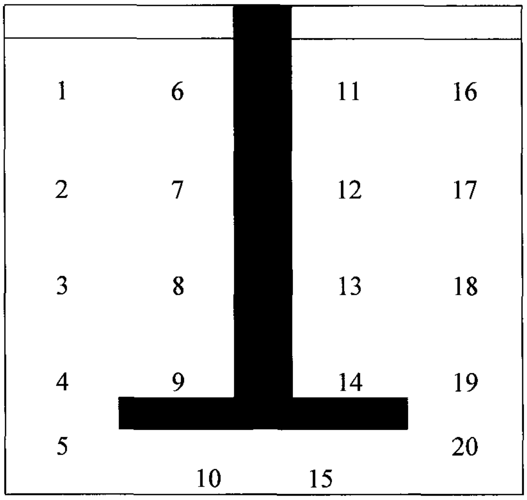

Figure 2.3 Locations of 20 sampling points for mixing time determination analyzed by the colorimetric method.

2.5 Mixing Time Determination at Different Rotational Speeds

In this work, the agitation speed was varied from 100 rpm to 200 rpm, in 25 rpm increments. At speeds higher than 200 rpm the mixing tank showed signs of mechanical distress, since this tank was made of a thin plastic wall instead of glass. When the speed was higher than 200 rpm, the bottom of the tank appeared to implode and the wall was slightly squeezed by high shear mixing within the tank.

All experiments were performed in the turbulent regime as indicated by the Reynolds number (Re) defined as:

$$\mathrm{Re} = \frac{\rho N D_2}{\mu} \qquad (2)$$

The flow regime for a baffled system is characterized by the Re number as follow;

$\mathrm{Re} < 10$	Laminar regime
$10 < \mathrm{Re} < 10{,}000$	Transition regime
$\mathrm{Re} > 10{,}000$	Turbulent régime

Speed (rpm)	Reynolds number (Re)
100	80353.6
125	100442.0
150	120530.4
175	140618.8
200	160707.2

Table 2.1 Corresponding Reynolds number to different rotational speeds

2.6 Data Analysis

The result of this work are typically displayed by plotting the normalized conductivity output (when the conductivity method was used) or normalized light intensity mentioned (when the colorimetric method was used), as described by Equation (1), as a function of time. In addition, the results are presented as mixing time θ_{95} vs. impeller speed N, as non-dimensional mixing time, $\theta_{95}N$, vs. N.

A review of the literature shows that the non-dimensional mixing time in baffled systems is typically only a function of geometric parameters, such as impeller type, impeller diameter-to-tank diameter ratio (D/T) and impeller off-bottom clearance-to-diameter ratio (C/T). Therefore, for a given geometry the non-dimensional mixing time in baffled systems is typically a constant:

$$\theta_D N = \text{constant} \qquad (3)$$

This work employed 95% mixing time (θ_{95}) as a mixing time. So that equation (3) would become for *baffled* systems:

$$\theta_{95} N = \text{constant} \qquad (4)$$

However, no information is available in the literature for unbaffled or partially baffled systems. Therefore, the applicability of this approach to the systems studied in this work is questionable at the moment.

CHAPTER 3

RESULTS

3.1 Mixing Time in the Unbaffled Tank Obtained with the Conductivity Method

3.1.1 Mixing Time in the Unbaffled Tank Obtained with One Probe Located at the Wall

The mixing time obtained in the unbaffled tank with the conductivity method at an agitation speed of 100 rpm was found to be 248.23 s (averages of three experiments with standard deviation of 7.61%). Figure 3.1 shows that the normalized conductivity output gradually increased from zero and stabilized within the range of 0.95 and 1.05 representing θ_{95}. It was visually observed that near the wall where the probe was placed the flow of water was disturbed by the presence of the probe, creating a secondary flow toward to the vortex region near the mixing shaft.

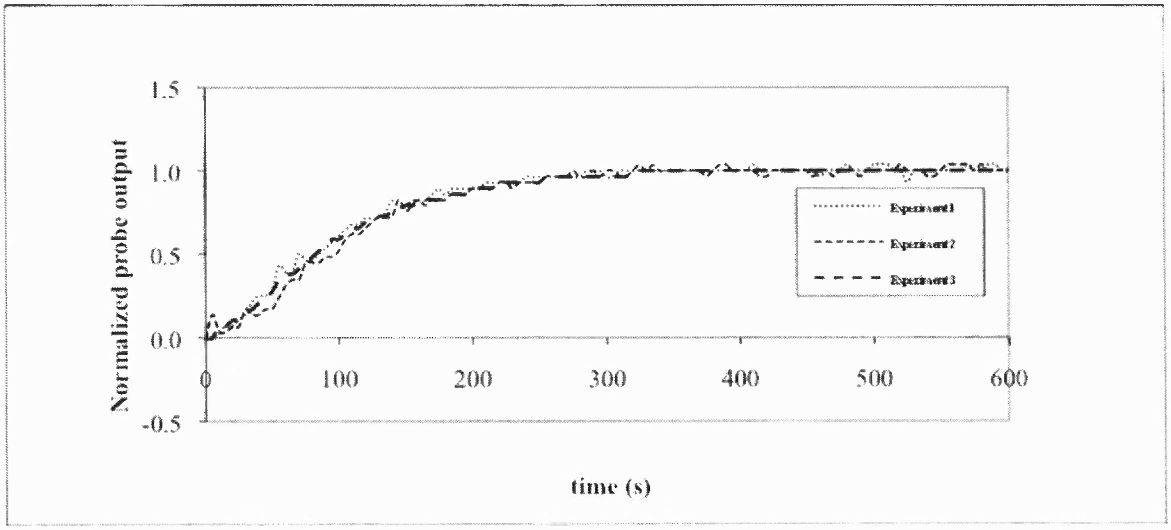

Figure 3.1 Experimental normalized conductivity for the unbaffled tank with the probe at the wall (N=100 rpm).

3.1.2 Mixing Time in the Unbaffled Tank Obtained with One Probe Located Midway between the Wall and the Shaft

The mixing time obtained with the conductivity method after the tracer was injected at an agitation speed of 100 rpm was found to be 76.61 s (averages of three experiments with standard deviation of 5.7%). The normalized conductivity outputs shown in Figure 3.2 were initially high and dropped sharply before the curve increased to reach the value of 1.0. When the probe was placed midway between the shaft and the wall, the water flow at the surface was split into two directions, i.e., toward the shaft and toward the wall. The vortex was still observed in this experiment.

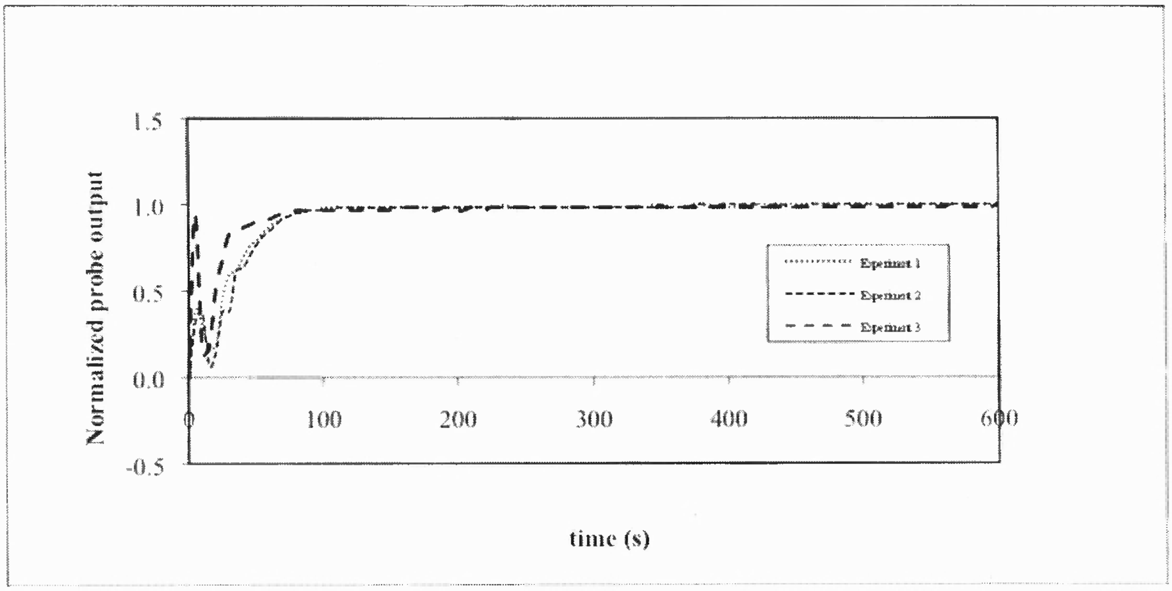

Figure 3.2 Experimental normalized conductivity for the unbaffled tank with the probe located midway between the wall and the shaft (N=100 rpm).

3.1.3 Mixing Time in the Unbaffled Tank Obtained with Two probes Located at the Wall (Position 1) and Midway between the Wall and the Shaft (Position 2)

The mixing time was significantly reduced in the system in which two probes were placed simultaneously. The mixing times measured by the probe in Position 1 and Position 2 were 27.37 s and 47.50 s respectively, with standard deviations of 0.2% and 2.8% respectively). Figure 3.3 shows that the normalized conductivity output obtained from the probe located at Position 1 gradually rose until it reached the value of 1.0. The output in Figure 3.4 displaying the normalized conductivity output obtained from the probe located at Position 2 increased sharply with considerably higher normalized value (maximum is 2.34), and then decreased to 1.0. Even when two probes were used the probe at Position 2 produced a flow change near the surface by diverting the water stream to the shaft and the wall. Similarly the probe at Position 1 created a flow toward the shaft region. The shape vortex of the vortex was smaller compared to that where one probe was placed regardless of position.

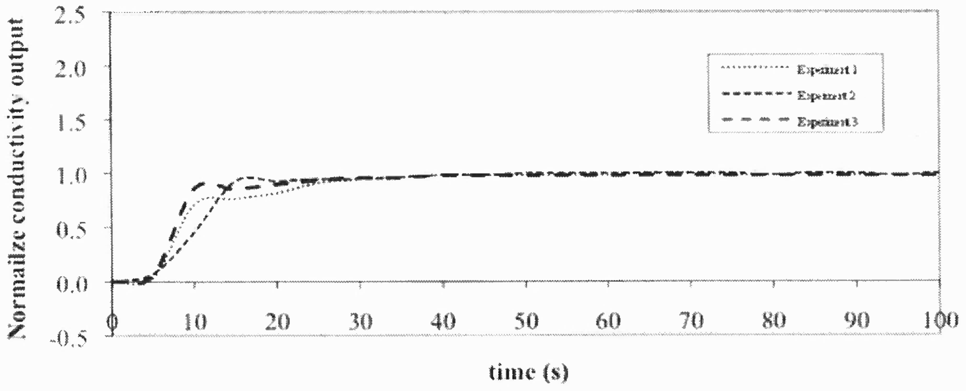

Figure 3.3 Experimental normalized conductivity (in the presence of two probes) for the unbaffled tank with the probe located at wall (N=100 rpm).

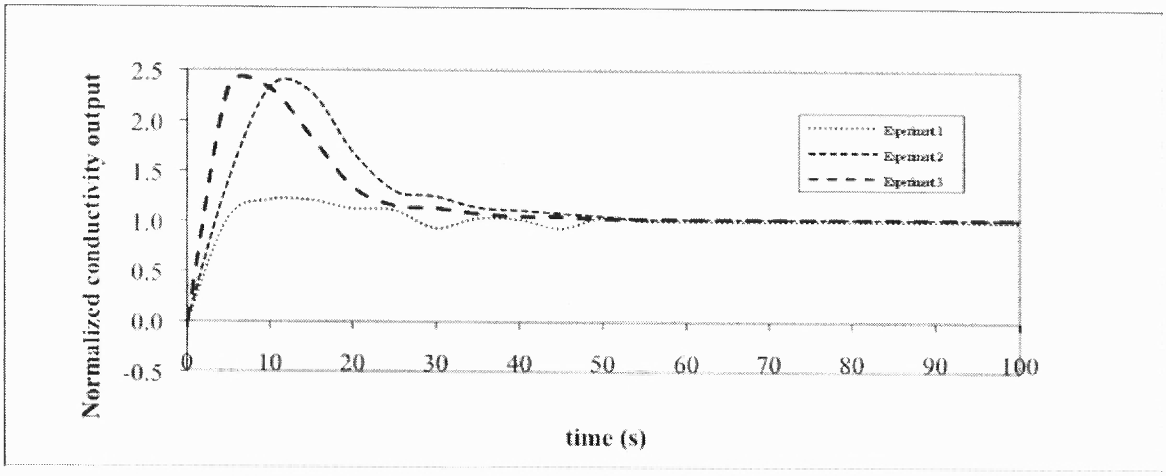

Figure 3.4 Experimental normalized conductivity (in the presence of two probes) for the unbaffled tank with the probe located midway between the wall and the shaft (N=100 rpm).

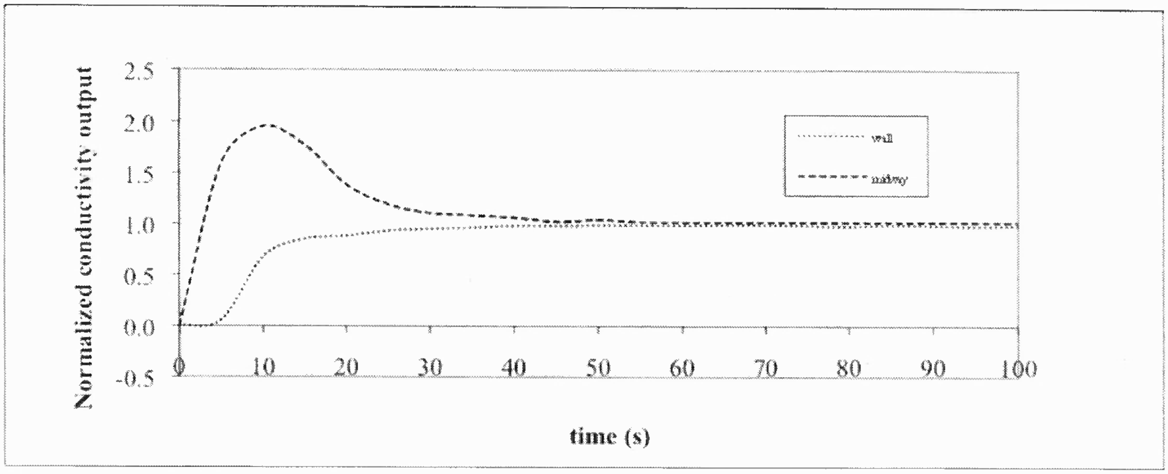

Figure 3.5 Average of experimental normalized conductivity in which probes were Located at the wall (Position 1) and midway between the wall and the shaft (Position 2) (N=100 rpm).

3.2 Mixing Time in the Unbaffled Tank Obtained with the Colorimetric Method

3.2.1 Mixing Time in the Unbaffled Tank in the Absence of a Probe

Figure 3.6 shows the colorimetric output at one sampling location (Location 1) when no probes were present. The output started at a value corresponding to the light intensity when the solution was entirely pink and eventually reached the final level corresponding to a completely colorless solution. At each sampling point, the mixing time was the average of the results of three experimental replicates. The mixing time measured with this method was found to be 179.28 s (average of 20 points with standard deviation of 0.9%). Figure 3.7(a) displays the individual mixing time of 20 sampling points by using the RGB function analysis in the MATLAB application. More rapidly mixed regions (producing lower mixing time) were found to be at the wall and above the impeller.

It was visually observed that the color in the experiments shown in Figure 3.7(b) first began to change from pink to colorless in the region below the impeller (Region 1). Next, the color changed upward along the wall (Region 2). The region above the impeller (Region 3) was the last region where decolorization occurred. Decolorization progressed above the impeller up to the liquid surface.

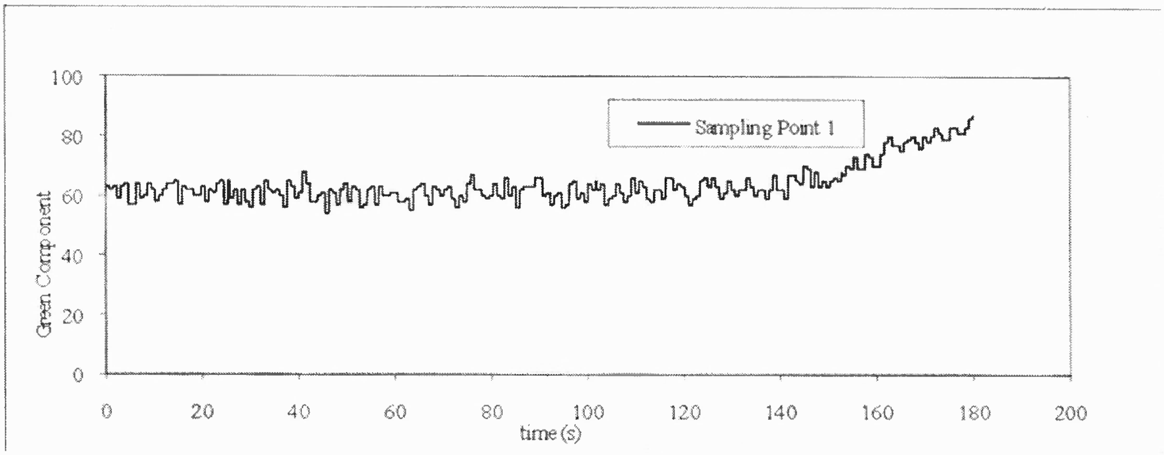

Figure 3.6 Green component output obtained with colorimetric method at sampling point 1 with absence of conductivity probe.

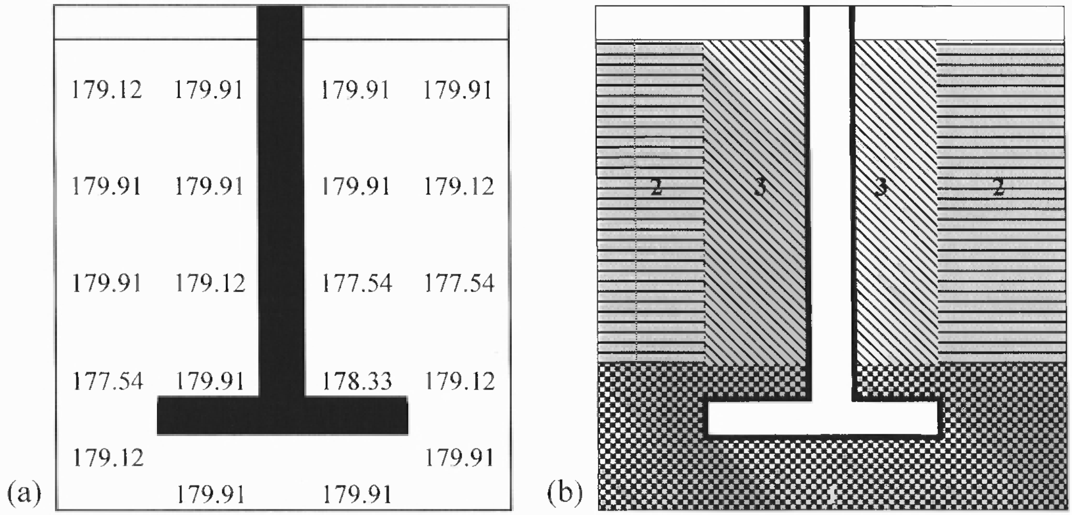

Figure 3.7 (a) Individual mixing times obtained with the colorimetric method in absence of conductivity probe
(b) sequence in which regions changed color in absence of conductivity probe
System: unbaffled tank; Agitation speed= 100 rpm.

3.2.2 Mixing Time in the Unbaffled Tank in the Presence of One Probe Located at the Wall

Figure 3.8 shows the colorimetric output at one sampling location (Location 1) when one probe at the wall was present. The mixing time obtained with the colorimetric method using image processing analysis when the agitation speed was 100 rpm and one probe was placed 15 mm from the wall was observed to be 121.07 s (average of 20 points within the tank with a standard deviation of 1.6%). Figure 3.9 displays the individual mixing times at the 20 sampling locations. More rapidly mixed regions (shorter mixing times) were found to be on the impeller plane, where the mixing time was 117.47 s. From visual observation, the color evolution pattern was similar to that in the absence of a probe. Visual observation of the color evolution was also similar to that found in the experiments in the absence of probe.

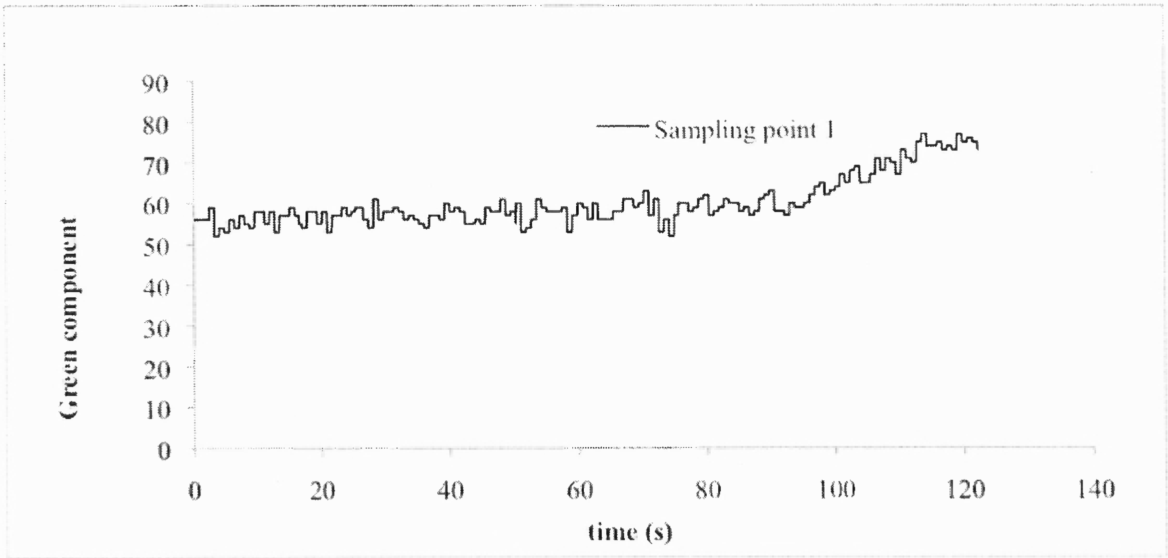

Figure 3.8 Green component output obtained with colorimetric method at sampling point 1 with presence of one conductivity probe at wall.

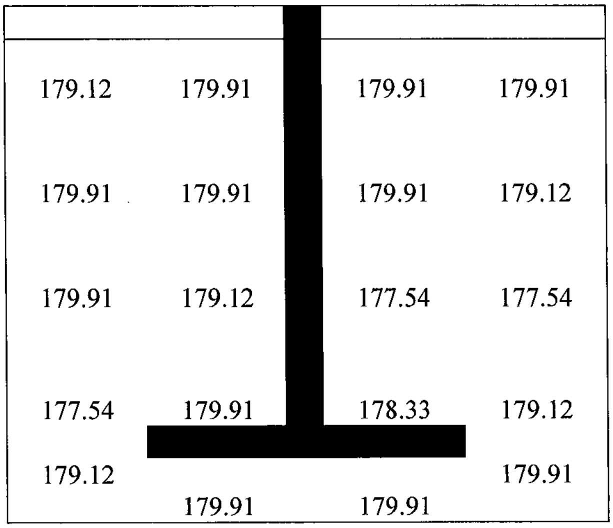

Figure 3.9 Individual mixing times obtained with the colorimetric method in presence of conductivity probe at the wall. System: unbaffled tank; Agitation speed= 100 rpm.

3.2.3 Mixing Time in the Unbaffled Tank in the Presence of Two Probes Located at the Wall and Midway between the Wall and the Shaft

Figure 3.10 shows the colorimetric output at one sampling location (Location 1) when two probes were present. When both probes were present, the color changed from pink to colorless within approximately 25 s. The actual mixing time using image processing analysis was determined to be 24.28 s (average of 20 points with standard deviation of 1.2%). The results from image analysis shown in Figure 3.11 reveals that the right region on the same plane of the impeller was the first to achieve the desired level of uniformity, with the mixing time of 20.83 s w. Visual observation of the color evolution was also similar to that found in the experiments in the absence of probe.

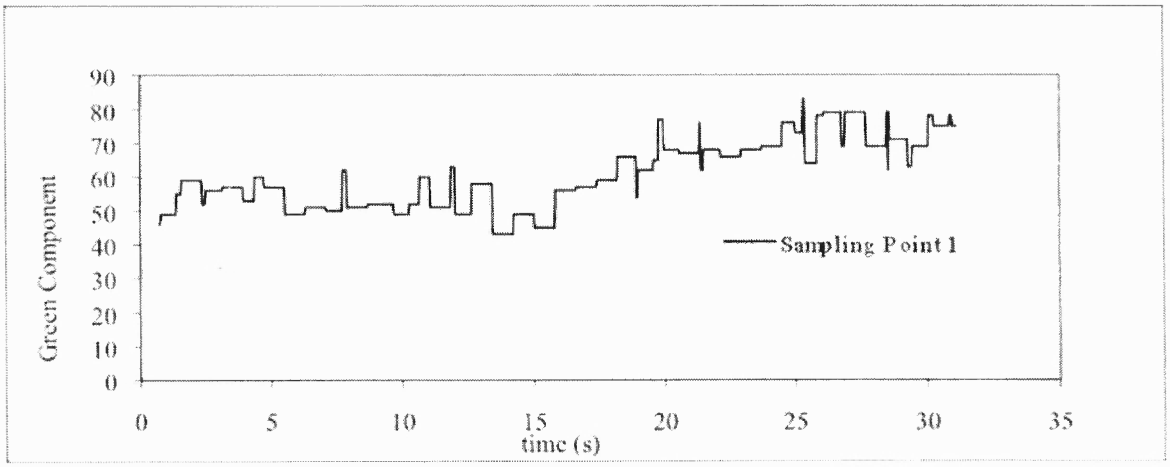

Figure 3.10 Green component output obtained with colorimetric method at sampling point 1 with presence of two conductivity probes.

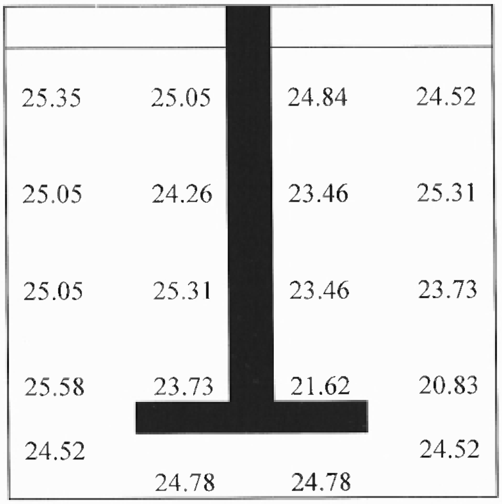

Figure 3.11 Individual mixing time obtained with the colorimetric method in the presence of two probes located at the wall and midway between the wall and the shaft. System: unbaffled tank; Agitation speed= 100 rpm.

3.3 Mixing Time in the Unbaffled Tank at Different Agitation Speeds

In these experiments, the agitation speed was varied from 100, to 200 rpm in 25 rpm increments. A small vortex was observed at 100 rpm. The depth and size of this vortex increased with increasing agitation speed. A summary of the mixing time results is presented in Table 3.1. The same results, reported in Figure 3.12, shows that the mixing time is inversely proportional to agitation speed. From the speed of 100 rpm to 125 rpm, the mixing time decreased by nearly 50% (248.23 s vs. 123.38 s). The mixing time slightly decreased when the speed was varied from 125 rpm to 175 rpm. At the two highest speeds tested here, i.e., 175 rpm and 200 rpm, the mixing time was very similar (i.e., 65.72 s and 67.10 respectively).

A 2nd-order polynomial equation was used to fit the data, as shown in Figure 3.12. The resulting correlation is as follow:

$$\theta_{95} = y = 0.0279N^2 - 10.043N + 965.01$$

The non-dimensional mixing number, $\theta_{95}N$ shown is Figure 3.13 was in the range of 190-260 with the exception of the experiment at 100 rpm for which $\theta_{95}N$ was found to be 413.7.

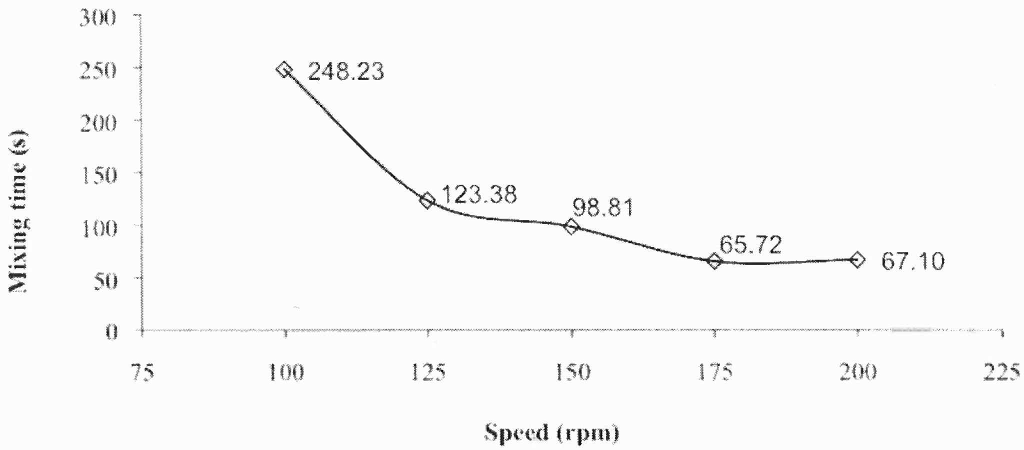

Figure 3.12 Plot of mixing time as a function of agitation speed under unbaffled conditions.

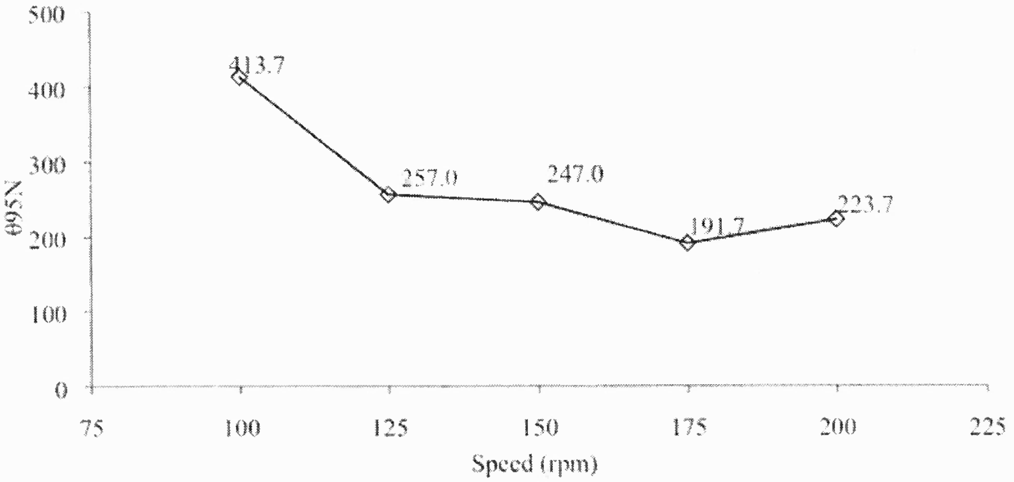

Figure 3.13 Plot of $\theta_{95}N$ as a function of agitation speed under unbaffled conditions.

Speed	Reynolds number	Mixing time (s)			
		Experiment	Regression	%error	
(rpm)	(Re)		Prediction		$\theta_{95}N$
100	80353.6	248.23	239.71	3.43	413.72
125	100442.0	123.38	145.57	-17.99	257.04
150	120530.4	98.81	86.31	12.65	247.03
175	140618.8	65.72	61.92	5.78	191.68
200	160707.2	67.10	72.41	-7.91	223.67

Table 3.1 Summary of experimental mixing time, regression predicted mixing time, and $\theta_{95}N$ obtained from different rotational speeds experiment under unbaffled condition.

3.4 Mixing Time in the Partially Baffled Tank at Different Agitation Speeds

The results for mixing time as a function of agitation speed for the case of the tank baffled with a single beavertail baffle are shown in Figure 3.14 and in Table 3.2. The data show that the mixing time is inversely proportional to agitation speed. At 100 rpm, the mixing time was found to be 31.06 s while at the highest speed investigated here (i.e, 200 rpm) the mixing time was 8.90 s. Under baffled condition, the mixing time linearly decreased with increasing speed from 100 rpm to 200 rpm.

The regression equation for mixing time as a function of the impeller speed (Figure 3.14) was linear and the correlation can be established as follow:

$$\theta_{95} = -0.2238N + 52.976$$

This equation was used to predict the mixing times shown in Table 3.2.

The non-dimensional mixing number $\theta_{95}N$ shown in Figure 3.15 was relatively constant (38–51) when N was in the range 100-175 rpm. However, $\theta_{95}N$ at the maximum agitation speed studied here (200 rpm) was 29.7. Although the tank was partially baffled with a beavertail baffle, the vortex was still observable even at speeds as low as 100 rpm. This vortex became bigger as the agitation speed increased.

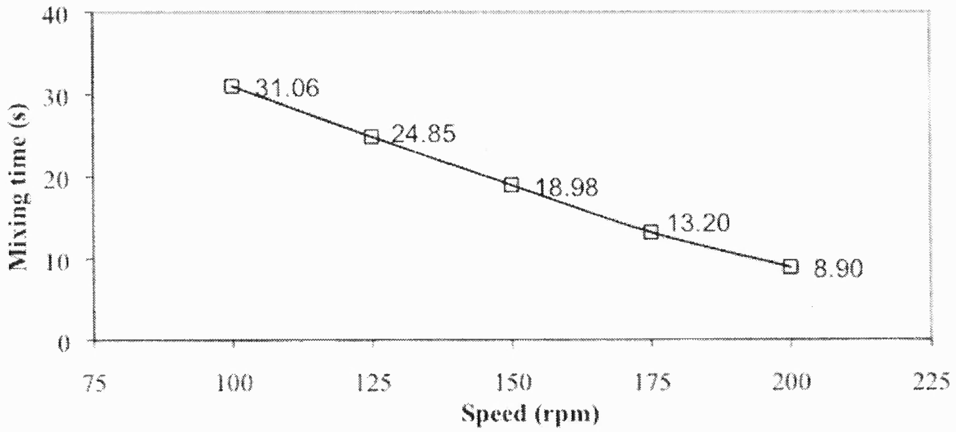

Figure 3.14 Plot of mixing time as a function of agitation speed under partially baffled conditions.

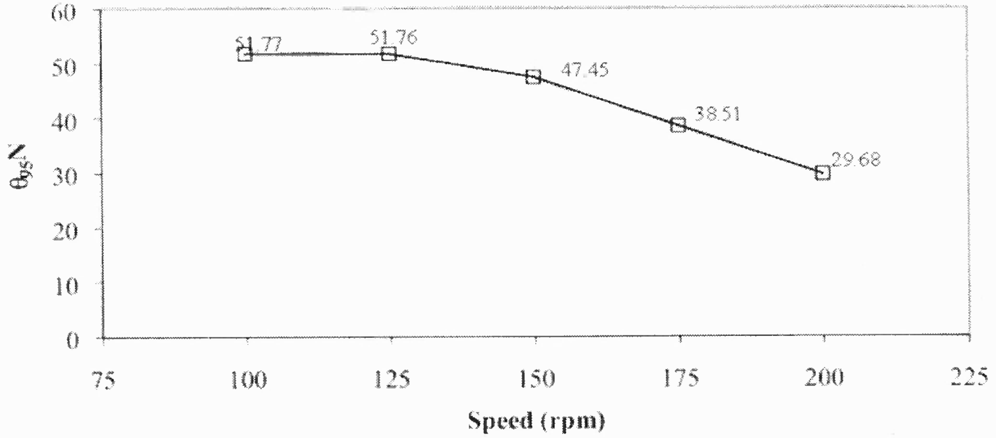

Figure 3.15 Plot of $\theta_{95}N$ as a function of agitation speed under partially baffled conditions.

		Mixing time (s)			
Speed (rpm)	Reynolds number (Re)	Experiment	Regression Prediction	%error	$\theta_{95}N$
100	80353.6	31.06	30.60	1.51	51.77
125	100442.0	24.85	25.00	-0.63	51.76
150	120530.4	18.98	19.41	-2.24	47.45
175	140618.8	13.20	13.81	-4.60	38.51
200	160707.2	8.90	8.22	7.73	29.68

Table 3.2 Summary of experimental mixing time, regression predicted mixing time, and $\theta_{95}N$ obtained at different agitation speeds under partially baffled conditions.

3.5 Mixing Time in the Fully Baffled Tank at Different Agitation Speeds

No vortex was observed at every varied speed in this experiment. During the mixing, the surface of water was flat even though the speed was increased to 200 rpm. The results for mixing time as a function of agitation speed for the case of the tank baffled with fully baffle are shown in Figure 3.16 and in Table 3.3. The data show that the mixing time is inversely proportional to agitation speed. At 100 rpm, the mixing time was found to be 14.33 s while at the highest speed investigated here (i.e, 200 rpm) the mixing time was 7.27 s. Under fully baffled condition, the mixing time linearly decreased with increasing speed from 100 rpm to 200 rpm.

The regression equation for mixing time as a function of the impeller speed (Figure 3.16) was linear and the correlation can be established as follow:

$$\theta_{95} = -0.073N + 21.232$$

This equation was used to predict the mixing times shown in Table 3.3.

The non-dimensional mixing number $\theta_{95}N$ shown in Figure 3.17 was relatively constant (23-26) for every speed.

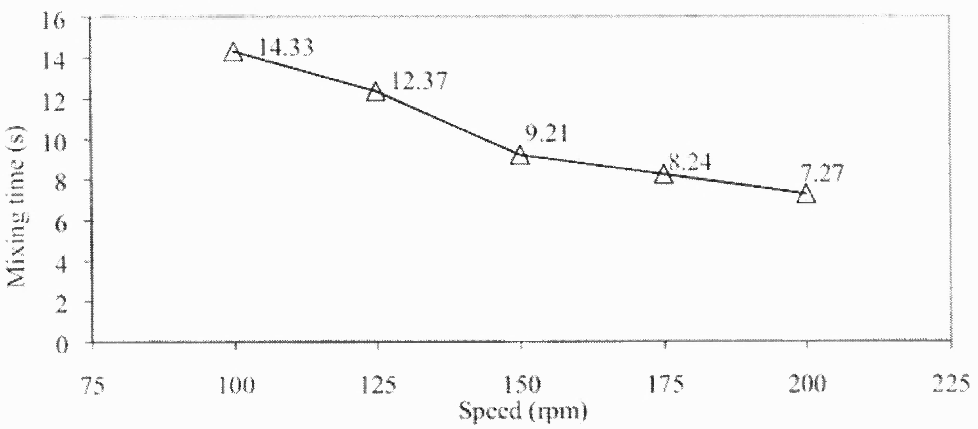

Figure 3.16 Plot of mixing time as a function of agitation speed under fully baffled conditions.

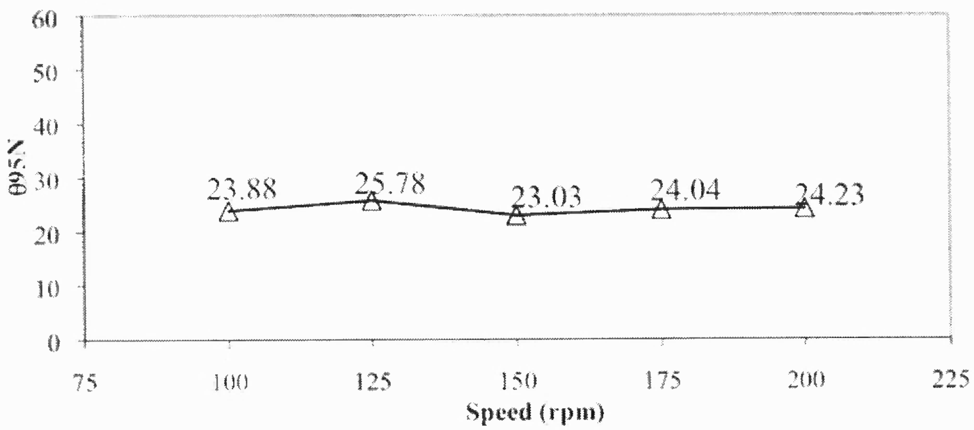

Figure 3.17 Plot of $\theta_{95}N$ as a function of agitation speed under fully baffled conditions.

Speed (rpm)	Reynolds number (Re)	mixing time (s)			$\theta_{95}N$
		Experiment	Regression Prediction	%error	
100	80353.6	14.33	13.93	2.75	23.88
125	100442.0	12.37	12.11	2.15	25.78
150	120530.4	9.21	10.28	-11.61	23.03
175	140618.8	8.24	8.46	-2.62	24.04
200	160707.2	7.27	6.63	8.77	24.23

Table 3.3 Summary of experimental mixing time, regression predicted mixing time, and $\theta_{95}N$ obtained at different agitation speeds under fully baffled conditions.

CHAPTER 4

DISCUSSION

4.1 Comparison of Mixing Time Results Using Different Determination Methods

4.1.1 Effect of the Presence of One Conductivity Probe at the Wall in the Unbaffled System

In the unbaffled system and in the presence of a single probe at the wall the mixing time results obtained with the two detection methods were not in agreement. The mixing time obtained with the conductivity method was more than twice that obtained with the colorimetric method. This shorter mixing time may arise from inappropriate endpoint determination. Visual inspection was performed by using a stopwatch to determine the mixing time. The stopwatch was started when the acid solution was injected into the tank and was stopped as the final pink color region changed to colorless. This monitoring duration was also applied to video taping. If the video recording has been keeping until 250 s, the normalized output might reveal more accurate endpoint.

Furthermore, the colorimetric results in this work were less reproducible. Seven replicates were performed and four out of seven experiments had similar mixing times (when the last pink region completely changed to colorless), which was approximately 120 s. Other results were 140 s, 177 s, and 196 s. This poor reproducibility could be attributed to two reasons. The first reason was the initial condition in each experiment. Distilled water in the tank was not discarded after every experiment in order to run a new set of experiments with limited distilled water. Between experiments, an NaOH solution was added to neutralize the acid conditions in the tank and bring the pH back to the base condition, as determined by a pH meter. The pH so obtained may have varied slightly resulting in slightly different starting points. The second reason could also be attributed to unchanged distilled water.

In addition, another limitation could come from the analysis of the RGB component featured in the MATLAB software application. A single file cannot contain more than 1,000 frames. Taping was recorded in AVI format (30 frames/s), implying that the maximum recording time per file could not exceed 33.33 s. To analyze the entire video captured for the one-probe case, the AVI file was split into 5 files and a separate RGB analysis was conducted for each file. Twenty sampling points were identically selected by locating the same coordinate in each split file. At most locations it was found that the initial value of the G component in the new file was slightly different that the corresponding last value of the same component in the previous file. For example, in Experiment #5, the total recorded time was 118.47 s. Thus, the video was cut into 5 files. At Sampling Point 15, the value of the final G component obtained from the first split file was 104, but the first G component obtained from the second split file was found to be 99. It could have been that the color indeed changed at that second, but this seems unlikely. In addition, such rapid changes were found at most sampling points. Nevertheless, this circumstance can only explain errors within the total captured video (118.47 s), and not why the mixing time was considerably less than the mixing time obtained with the conductivity probe technique.

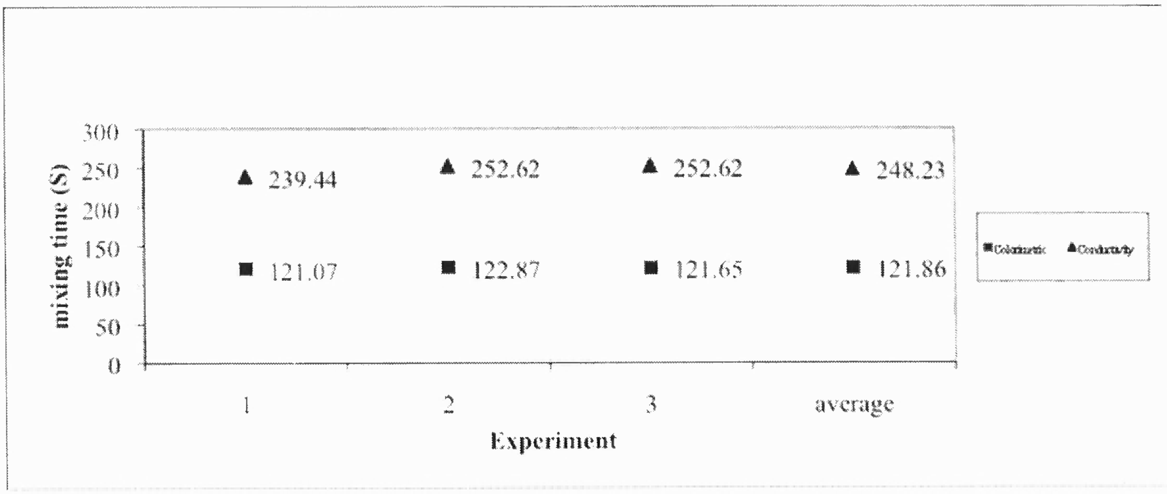

Figure 4.1 Comparison of three experiments in which the mixing time was obtained by the conductivity method and colorimetric method in the presence of one probe located at the wall.

4.1.2 Effect of the Presence of Two Conductivity Probes in the Unbaffled System

Figure 4.2 shows that both measuring methods produced similar mixing times, both only as far as the location at the wall is concerned. In such as case, the average mixing times obtained with the conductivity method and the colorimetric method were 27.37 s and 24.29 s, respectively. Figure 4.3 shows that at the probe between the wall and the shaft the mixing time was much longer when the conductivity method was used than when the colorimetric method was used.

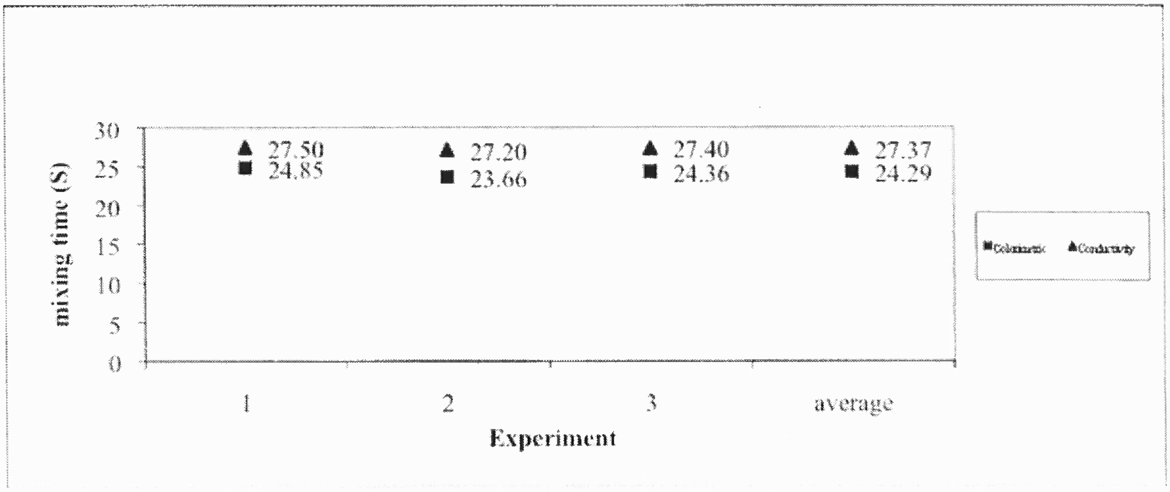

Figure 4.2 Comparison of three experiments in which the mixing time was obtained with the conductivity method and the colorimetric method in the presence of two probes in the tank.

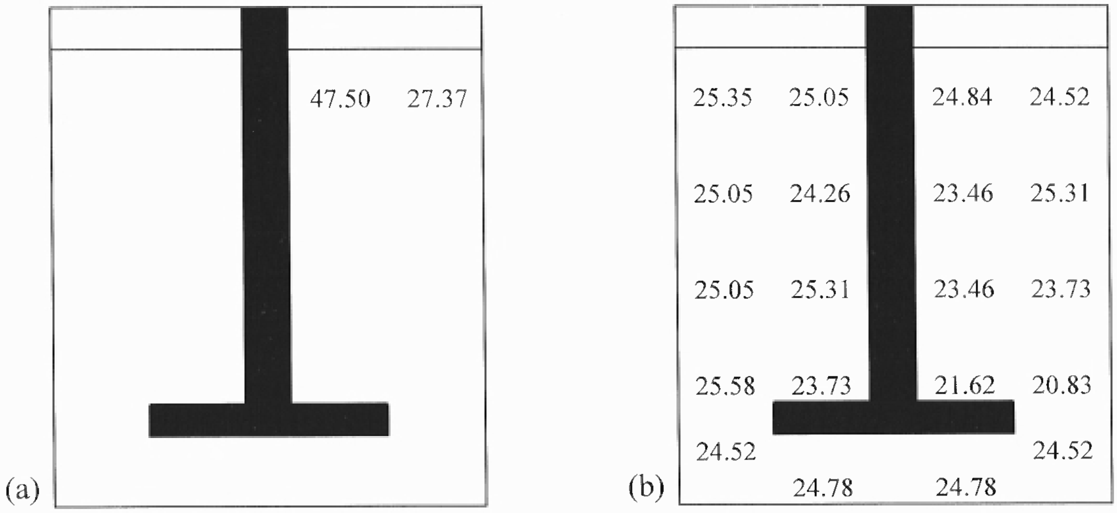

Figure 4.3 Comparison of mixing time at individual monitoring point in the presence of two probe located in the tank: (a) conductivity method (b) colorimetric method.

4.2 Comparison of Mixing Times in Unbaffled Tanks in the Presence of Different Number of Probes

4.2.1 Results Obtained with the Conductivity Method

Three set of experiments in the unbaffled tank were conducted using the conductivity method, i.e., in presence of one probe at the wall, one probe located midway between the wall and the shaft, and with two probes at the two previous investigation points. With one probe at the wall, the mixing time obtained by using the conductivity method with this probe was comparatively long (248.23 s). When only the probe located midway between the wall and the shaft was installed the mixing time was much shorter (76.61 s). Finally, when both probes were installed and they both measured conductivity the mixing time measured near the wall was only 27.4 s while that in the center was 47.5 s (Figure 4.4). The results obtained with the probe at the wall are in close agreement with those obtained with the colorimetric method when both probes were present. The results imply that the introduction of the second probe at the midway position had a significant impact on the mixing time at the wall, reducing mixing time from 248.23 s to 27.37 s. The second probe obviously acted as the baffle in the system. This observation was interesting due to the fact that baffles are typically placed near the wall rather than midway between the wall and the shaft. Furthermore, the diameter of the conductivity probe (15.3 mm) is much smaller than the that of beavertail baffle employed in this work. Interestingly, a comparison between the mixing time obtained in the presence of two probes in the unbaffled tank and the mixing time in the partially baffled tank shows that both mixing times are very similar. The position of the probe placed in the system is assumed to have the effect on the mixing time because it directly alters the flow. Varying the probe position along the radius could possibly result in different mixing times. In addition, adding another baffle is expected to reduce the mixing time because results clearly showed decrease mixing time as more either the probe or baffle was introduced to the system.

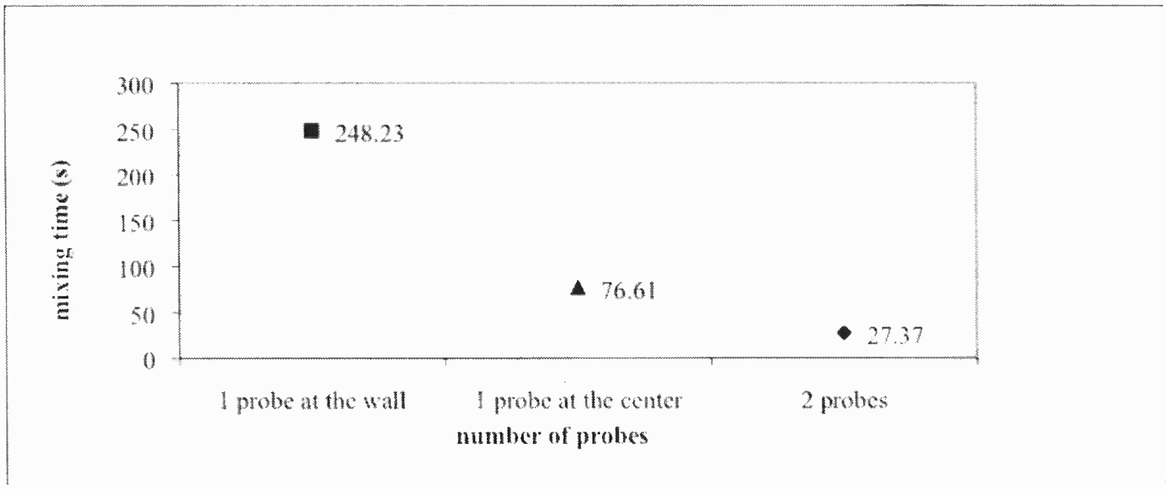

Figure 4.4 Experimental mixing time for different number and positions of the conductivity probes in the tank using the conductivity method (unbaffled condition; 100 rpm). When two probes were in place the mixing time in the figure refers to that measured near the wall.

4.2.2 Results Obtained with the Colorimetric Method

Despite the mixing time value in one probe sited at the wall experiment was not in agreement with the conductivity technique, Figure 4.5 shows that the mixing time measured with the colorimetric method decreased as the number of probes increased from one to two. The value measured with this method when the wall probe was present was significantly smaller than the corresponding mixing time measured with the conductivity method. However, the colorimetric method relies on measurements that involve the whole content of the tank and now just one point, as in the conductivity method. When the second probe was introduced, both methods gave similar results. These results confirm that the introduction of the second probe midway between the wall and the shaft produced a significant baffling effect.

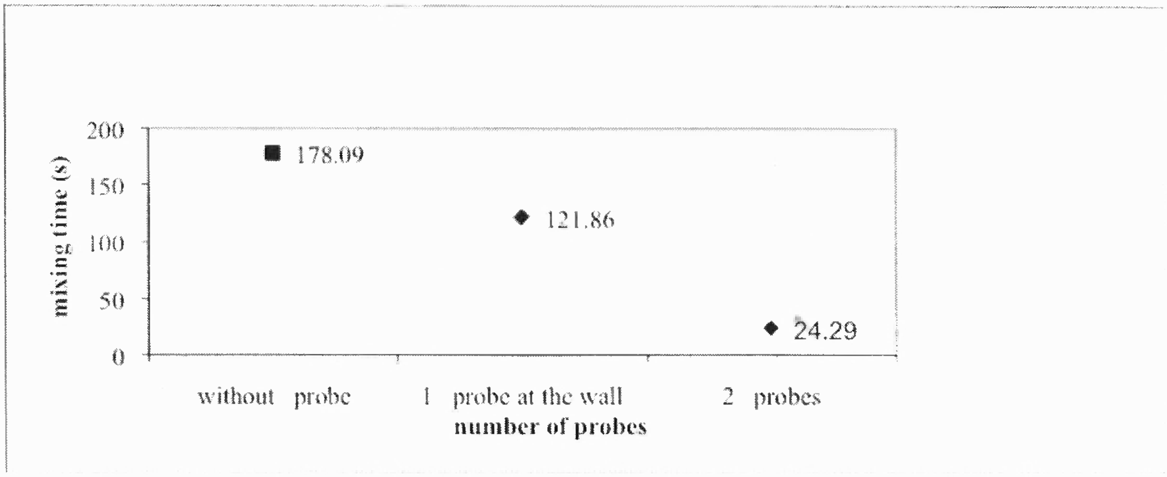

Figure 4.5 Experimental mixing time for different number and positions of the conductivity probes in the tank using the colorimetric method (unbaffled condition; 100 rpm). When two probes were in place, the mixing time in the figure refers to that measured near the wall.

Figure 4.6 (a-b) displays the mixing time at individual sampling point using the colorimetric method. The mixing times at all points are quite similar to each other. On the other hand, visual inspection showed that, regardless of probe location, the region under the impeller plane was the first area in which the color transition from pink to colorless began, followed by the region along the wall (from the impeller upwards toward the surface). Finally, the region above the impeller but within the circulation loop was the last zone where the pink color turned colorless. This is shown in Figure 4.6 (c-d). This implies that above color changing process cannot be fully differentiated by colorimetric method. There are several factors affecting an accuracy of image processing, such as the light intensity. Once the video was on the computer screen, the entire tank plane in the captured video was not evenly pink because there was some reflection spot on the tank plane.

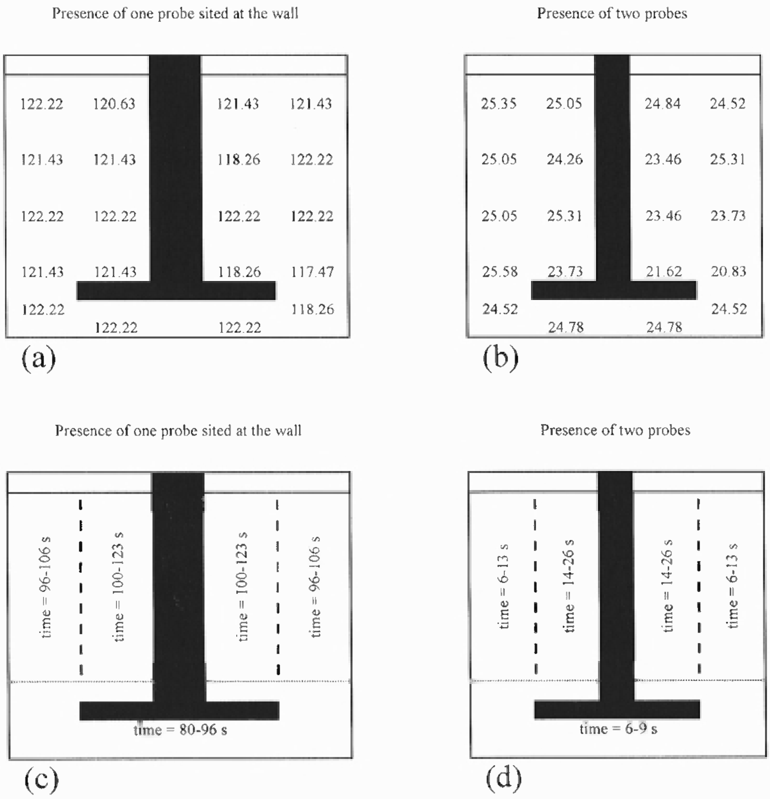

Figure 4.6 Comparison of mixing time at different locations in the tank using image processing and visual inspection (unbaffled condition):

(a) experiments with one probe located at the wall (image processing)
(b) experiments with two probes (image analysis)
(c) experiments with one probe sited at the wall (visual inspection)
(d) experiments with two probes (visual inspection).

4.3 Non-dimensional Mixing Time Number

Under unbaffled condition, $\theta_{95}N$ was calculated and it was found to be somewhat constant the agitation speed range of 125 rpm to 200 rpm. At 100 rpm, $\theta_{95}N$ was out of range with the value of 413.7 even though the Reynolds number stated that the system was in turbulent regime. The reason why $\theta_{95}N$ is not constant in these experiments is because the tank was unbaffled. Furthermore, a vortex was observed in this system at all speeds.

The value of $\theta_{95}N$ for partially baffled system was lower and less affected by agitation speed. However, at 200 rpm, the highest speed investigated here, $\theta_{95}N$ was appreciably lower. In addition, at this speed a relatively large vortex was clearly observed and tank started to deform at the bottom under the impeller shear action. The system is obviously unstable at high agitation speed.

The value of $\theta_{95}N$ for fully baffled system was not affected by agitation speed. $\theta_{95}N$ was constant with a value of 23- 26. No vortex was observed in any speeds.

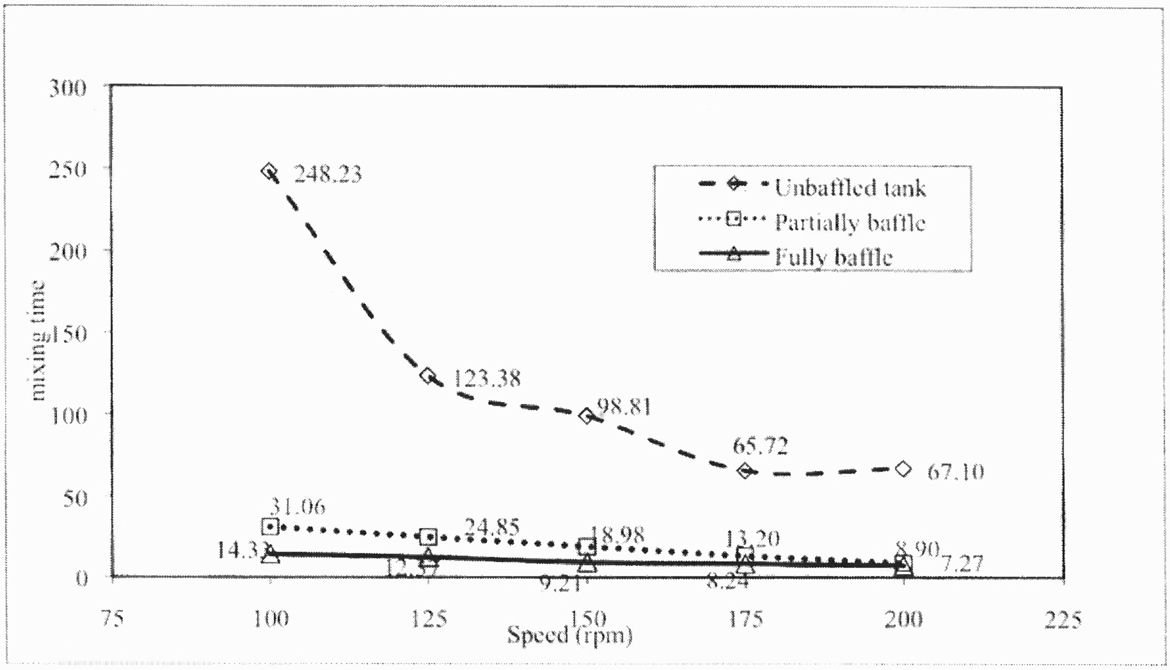

Figure 4.7 Effect of baffling on mixing time at different agitation speeds.

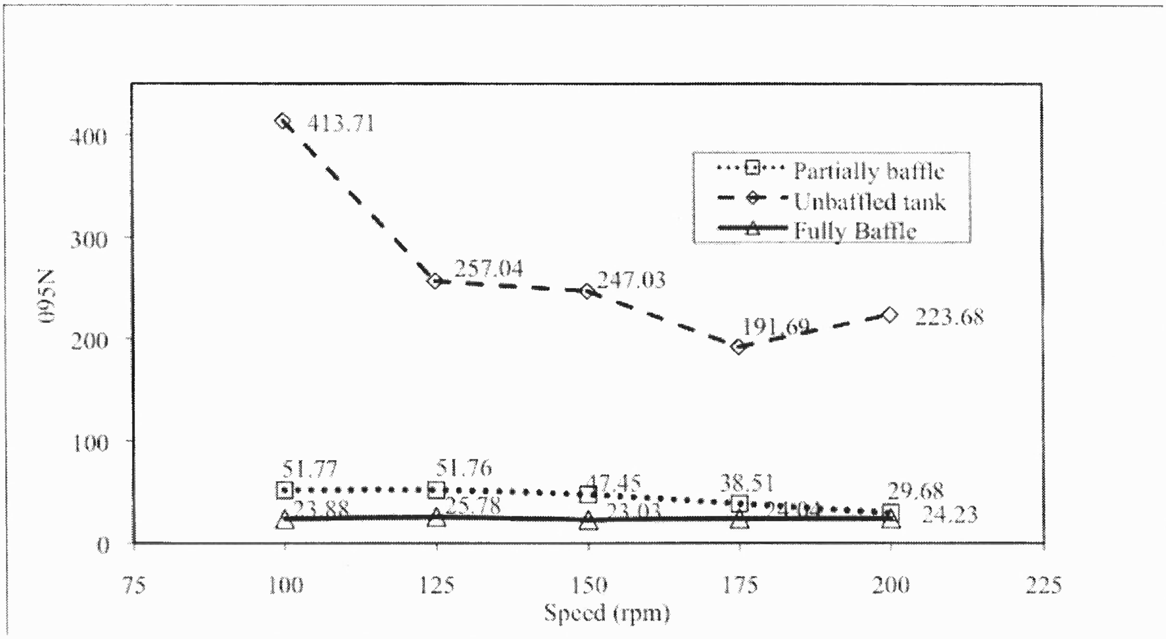

Figure 4.8 Effect of baffling on $\theta_{95}N$ at different agitation speeds.

CHAPTER 5

CONCLUSION

A number of conclusions can be drawn from this work:

- For the unbaffled system, different mixing times were obtained with the conductivity method depending on the location of the probe(s) and the number of probes. The colorimetric method produces results that are in agreement with the conductivity method only when two probes are used
- The unbaffled system appears to be extremely sensitive to minor geometric parameters, such as the presence or absence of the probes, their location and number, and the modality of the tracer addition
- For unbaffled tanks, the mixing time cannot be predicted using the conventional approach used for baffled systems
- The mixing time in partially baffled and fully systems is inversely proportional to rotational speed. The predicted mixing time from regression agrees well with the experimental results
- The non-dimensional mixing number, $\theta_{95}N$ in partially baffled system can be obtained within the speed range of 100 – 175 rpm. The $\theta_{95}N$ slightly decreased as speed increase.
- In fully baffled system, $\theta_{95}N$ was a constant number for every investigated speed, 100 – 200 rpm.

APPENDIX

MATLAB SOURCE CODES FOR DETECTION WITH RGB COMPONENT

MATLAB Source Code to Obtain the Picture from avi File

```
clear all
clc
close all

%
%save the movie as a Matlab file
vidObj=mmreader('directory of avi file');
images = read( vidObj );

%open the first picture and select the 20 points of interest
%for each point clic on Export data to workspace
%name of the point 'P1'

%display initial picture
Size=size(images);
picture=images(:,:,:,1);
image (picture)


%select the points then close the picture and start the second m-file
```

MATLAB Source Code to Extract Green Component (G) from Individual Sampling Point

```
% program to calculate the mixing time from a series of pictures taken with
% a regular camera
% The parameter used for tha analysis is the COLOR Intensity - generally
% the GREEN color intensity is the only one considered since it is less
% sensible to differences in external light

%clc
%clear all
%close all

%INPUT (msec!!!)
InjectionTime=5110;              %msec

RGB_tot=[];

%loop to take each picture from the movie
for i=1:Size(4)

picture=images(:,:,:,i);

%find the RGB component for each picture
%selected points


B=[P1.Position; P2.Position; P3.Position; P4.Position;
P5.Position;P6.Position;P7.Position;P8.Position;P9.Position;P10.Position; P11.Position;
P12.Position;P13.Position;P14.Position;P15.Position;P16.Position;P17.Position;P18.Position;P19.Position;P20.Position;];
RGB_pict=[];

%loop to analize all points
for y=1:20
    RGB=picture(B(y,2),B(y,1),:);
    RGB_pict=[RGB_pict;RGB];
end
RGB_tot=[RGB_tot RGB_pict];
end
%evolution of red component with time (columns) and points (rows)
R_tot=RGB_tot(:,:,1);
G_tot=RGB_tot(:,:,2);
B_tot=RGB_tot(:,:,3);

%%%%%%%%%%%%%%%%%%%%%%%%%%%%%%%%%%%%%%%%%%%%%%%%%%%%%%%%%%%%%%%%
%%%%%%%%%%%%%%%
%time vector definition

time (1)=0;
for i=2:Size(4)
  time(i)=time(i-1)+32.987288;
end

%%%%%%%%%%%%%%%%%%%%%%%%%%%%%%%%%%%%%%%%%%%%%%%%%%%%%%%%%%%%%%%%
%%%%%%%%%%%%%%%
```

REFERENCES

1. Dickey, D. S., Bittorf, K. J., Ramsey, C. J., Johnson, K. E., *Understand Flow Patterns in Glass-lined Reactors*, in *CEP*. 2004. p. 5.

2. Myers, K. J., Reeder M.F., Fasano, J. B. *Optimize Mixing by Using the Proper Baffles.* CEP 2002. **98**(2): p. 6.

3. Paul, E. L., Atiemo-Obeng, V. A, Kresta, S. M. *Handbook of Industrial Mixing.* 2004, Hoboken: John Wiley & Sons, Inc.

4. Cabaret, F., Bonnot, S., Fradette, L., Tanguy, P. A., *Mixing Time Analysis Using Colorimetric Methods and Image Processing.* Industrial & Engineering Chemistry Research, 2007. **46**: p. 11.

5. Armenante, P. M., Uehara Nagamine, E., *Effect of low off-bottom impeller clearance on the minimum agitation speed for complete suspension of solids in stirred tanks.* Chemical Engineering Science, 1998. **53**(9): p. 19.

6. Akiti, O., Yeboah, A., Bai, G., Armenante, P. M. *Hydrodynamic effects on mixing and competitive reactions in laboratory reactors.* Chemical Engineering Science, 2005. **60**: p. 14.

7. Rielly, C.D., Habib, M., Sherlock, J.-P. *Flow and Mixing Characteristics of a Retreat Curve Impeller in a Conical-based Vessel.* Chemical Engineering Research and Design, 2007.

8. Ge B., Armenante, P. M., Plank, R. V. *Experimental and Computational Determination of Blend Time in USP Dissolution Testing Apparatus II.* Journal of Pharmaceutical Sciences, 2007. **96**(11): p. 15.

9. Nagata, S., *Mixing Principles and Applications*. 1975, New York: Wiley.

10. Kappel, M., *Development and application of a method for measuring the mixture guality of miscible liquid. Application of the new method for highly viscous Newtonian liquids.* International Chemical Engineering, 1979. **19**: p. 571-590.